HHS Public Access

Author manuscript

J Physiol. Author manuscript; available in PMC 2021 October 01.

Published in final edited form as:

J Physiol. 2020 October ; 598(20): 4573–4590. doi:10.1113/JP280111.

S100A4 is activated by RhoA and catalyses the polymerization of non-muscle myosin, adhesion complex assembly and contraction in airway smooth muscle

Wenwu Zhang, **Susan J. Gunst**

Department of Anatomy, Cell Biology & Physiology, Indiana University School of Medicine, Indianapolis, IN, USA

Abstract

S100A4 binds to the heavy chain of non-muscle (NM) myosin II and can regulate the motility of crawling cells. S100A4 is widely expressed in many tissues including smooth muscle (SM), although its role in the regulation of their physiologic function is not known. We hypothesized that S100A4 contributes to the regulation of contraction in airway SM by regulating a pool of NM myosin II at the cell cortex. NM myosin II undergoes polymerization in airway SM and regulates contraction by catalysing the assembly of integrin-associated adhesome complexes that activate pathways that catalyse actin polymerization. ACh stimulated the interaction of S100A4 with NM myosin II in airway SM at the cell cortex and catalysed NM myosin filament assembly. RhoA GTPase regulated the activation of S100A4 via rhotekin, which facilitated the formation of a complex between RhoA, S100A4 and NM myosin II. The depletion of S100A4, RhoA or rhotekin from airway SM tissues using short hairpin RNA or small interfering RNA prevented NM myosin II polymerization as well as the recruitment of vinculin and paxillin to adhesome signalling complexes in response to ACh, and inhibited actin polymerization and tension development. S100A4 depletion did not affect ACh-stimulated SMmyosin regulatory light chain phosphorylation. The results show that S100A4 plays a critical role in tension development in airway SM tissue by catalysing NM myosin filament assembly, and that the interaction of S100A4 with NM myosin in response to contractile stimulation is activated by RhoA GTPase. These results may be broadly relevant to the physiologic function of S100A4 in other cell and tissue types.

Corresponding author S. J. Gunst: Department of Anatomy, Cell Biology and Physiology, Indiana University School of Medicine, 635 Barnhill Dr, Indianapolis, IN 46202, USA. sgunst@iupui.edu.

Author contributions

SJG and WZ conceived of the idea for the project. WZ and SJG designed the experiments. WZ conducted the experiments. WZ analysed the results. SJG supervised the data analysis. WZ wrote the paper with SJG. Both authors approved the final version of the manuscript submitted for publication and agree to be accountable for all aspects of the work. All persons designated as authors qualify for authorship, and all those who qualify for authorship are listed.

Additional information

Data availability statement

The data that support the findings of this study are available online in the supplementary material for this article. Details of the statistical analysis of data for each figure are provided in the Supporting Information.

Competing interests

The authors declare that they have no competing interests.

Supporting information

Additional supporting information may be found online in the Supporting Information section at the end of the article.

Keywords

cytoskeleton; myosin heavy chain; smooth muscle

Introduction

S100A4 is a member of the S100 family of low molecular weight (10–12 kDa) Ca^{2+}-binding proteins that function as calcium-activated switches to regulate the activity of diverse protein targets (Garrett *et al*. 2006; Boye & Maelandsmo, 2010; Donato *et al*. 2013; Gross *et al*. 2014; Ambartsumian *et al*. 2019). High levels of intracellular S100A4 are expressed in motile cell types such as immune cells, as well as in mesenchymal fibroblastic cells (Garrett *et al*. 2006; Li *et al*. 2010). S100A4 is also highly expressed in a multiple types of metastatic cancer cells and plays a significant role in the metastatic processes in these cells (Davies *et al*. 2002; Helfman *et al*. 2005; Garrett *et al*. 2006; Ambartsumian *et al*. 2019). The expression of S100A4 has also been demonstrated in smooth muscle (SM) cells and tissues; however its physiologic function in this tissue has not been determined (Lawrie *et al*. 2005; Brisset *et al*. 2007; Reimann *et al*. 2015).

S100A4 interacts directly with non-muscle (NM) myosin II to mediate directional cell movement at the leading edge of migrating cells. The overexpression of S100A4 in fibroblasts and epithelial tumor cells results in increased cell motility, whereas the ablation or reduction of S100A4 expression in tumor cells correlates with decreased cell motility (Helfman *et al*. 2005; Garrett *et al*. 2006; Li & Bresnick, 2006; Boye & Maelandsmo, 2010; Ambartsumian *et al*. 2019). There is evidence that S100A4 regulates macrophage motility through its effects on NM myosin IIA filament assembly (Li *et al*. 2010); however, there is little information regarding the function of S100A4 under normal physiologic conditions in other cells and tissues.

SM tissues express both the NM and SM isoforms of myosin II (Lofgren *et al*. 2003; Eddinger & Meer, 2007; Yuen *et al*. 2009; Zhang & Gunst, 2017). Although the role of SM myosin II as the primary motor for muscle contraction and tension generation is well-established, NM myosin II has also been shown to play an essential role in the regulation of airway SM contraction and tension development (Zhang & Gunst, 2017; Zhang *et al*. 2018). NM myosin II localizes to the cortex of the SM cell, where contractile stimulation induces the assembly of NM myosin monomers into filaments that interact with cortical actin and undergo activation and actomyosin cross-bridge cycling (Zhang & Gunst, 2017).

The contractile stimulation of airway SM tissues also catalyses the recruitment of proteins into signalling complexes at integrin-associated adhesion junctions (adhesomes). These signalling complexes regulate cytoskeletal dynamics and actin polymerization, as well as pathways to the nucleus that modulate phenotypic expression and protein synthesis (Opazo Saez *et al*. 2004; Zhang *et al*. 2005; Gunst & Zhang, 2008; Desai *et al*. 2011; Huang *et al*. 2011; Zhang *et al*. 2012; Zhang *et al*. 2015; Wu *et al*. 2016; Huang & Gunst, 2020). Both adhesome complex assembly and actin polymerization are essential steps in the process of tension development that occur in concert with the activation of actomyosin cross-bridge cycling by SM myosin II. NM myosin II filaments interact with actin at the cell cortex to

mediate the recruitment of cytoskeletal proteins to adhesome signalling complexes (Zhang *et al*. 2015; Zhang & Gunst, 2017; Zhang *et al*. 2018). The assembly and activation of non-muscle myosin II at the cortex of the SM cells is indispensable for contraction and tension development by airway SM tissues.

NM and SM myosin II molecules have a similar structure: two 230 kDa heavy chains with globular head domains that contain the ATP and actin-binding sites connected to an α-helical coiled-coil rod backbone that terminates in a short non-helical tail (Vicente-Manzanares *et al*. 2009). The sequences of NM and SM isoforms of myosin II are very similar, with the exception of the short C-terminal non-helical terminal tailpiece, which is isoform-specific and regulates filament assembly. A pair of 20 kDa regulatory light chains (RLC) that regulate the ATPase activity of the globular heads and a pair of essential light chains that stabilize the heavy chain structure are bound to the heavy chain backbone near the globular head domains. In both SM and NM myosin II, actomyosin cross-bridge cycling is activated by phosphorylation of the 20 kDa RLC (Bresnick, 1999; Li *et al*. 2003; Eddinger & Meer, 2007; Yuen *et al*. 2009; Heissler & Sellers, 2016).

S100A4 binds to the NM myosin IIA heavy chain near the C-terminal end of the coiled-coil domain and overlaps the extended assembly competent non-helical domain that regulates filament assembly (Li & Bresnick, 2006; Malashkevich *et al*. 2008; Kiss *et al*. 2012). There is no evidence that S100A4 can bind to SM isoforms of the myosin II heavy chain. *In vitro* protein studies using truncated constructs of the NM myosin II heavy chain have shown that S100A4 plays a role in the regulation of NM myosin II filament assembly (Li *et al*. 2003). We hypothesized that S100A4 might contribute to the regulation of tension development during SM contraction by regulating NM myosin II assembly.

We investigated the physiologic role of endogenous S100A4 in contractile tension development in response to ACh in airway SM tissues. Our results show that S100A4 is a key regulator of NM myosin filament assembly and tension development in airway SM, and that the interaction of S100A4 with NM myosin is catalysed by the activation of RhoA GTPase in response to contractile stimulation. These results may be broadly relevant to the physiologic function of S100A4 in other cell and tissues types.

Methods

Ethical approval

All procedures were in accordance with procedures approved by the Institutional Animal Care and Use Committee (IUCAC) of Indiana University School of Medicine under the National Research Council's Guide for the Care and Use of Laboratory Animals. The Indiana University Laboratory Animal Resource Centre (LARC) at Indiana University School of Medicine procured mongrel dogs (20–30 kg, either sex) from LBL Kennels (Reelsville, IN, USA). Animals were killed on the day of procurement by I.V. injection of Fatal-Plus (Vortech Pharmaceuticals, Ltd, Dearborn, MI, USA) (pentobarbital sodium 390 mg mL^{-1}; propylene glycol, 0.01 mg mL^{-1}; ethyl alcohol; 0.29 mg mL^{-1}; benzylalcohol (preservative), 0.2 mg mL^{-1}) at a dose of 0.3 mL kg^{-1}, in accordance with procedures approved by the IACUC of Indiana University School of Medicine. After death, a tracheal

segment was immediately removed and placed in physiological saline solution (PSS). All investigators understand the ethical principles under which the *Journal of Physiology* operates, and all work complies with these principles.

Preparation of SM tissues and measurement of force

A tracheal segment was immediately removed and immersed in PSS (composition in mM: 110 NaCl, 3.4 KCl, 2.4 $CaCl_2$, 0.8 $MgSO_4$, 25.8 $NaHCO_3$, 1.2 KH_2PO_4 and 5.6 glucose). Strips of tracheal SM (1.0 × 0.2 to 0.5 × 15 mm) were dissected free of connective and epithelial tissues and maintained within a tissue bath in PSS at 37°C. Force was measured during isometric contractions by attaching the tissues to Grass force-displacement transducers (Grass Instruments, West Warwick, RI, USA). Prior to the beginning of each experimental protocol, muscle length was increased to maintain a preload of 0.5–1.0 g, and tissues were stimulated repeatedly with 10^{-5} M ACh until stable responses were obtained. The force of contraction in response to ACh was determined before and after treatment with plasmids or other reagents.

Immunoblotting

For biochemical analysis, muscle tissues were rapidly frozen using liquid N_2-cooled tongs and pulverized in liquid N_2 using a mortar and pestle. Pulverized muscle strips were mixed with extraction buffer containing: 20 mM Tris-HCl at pH 7.4, 2% Triton X-100, 0.4% SDS, 2 mM EDTA, phosphatase inhibitors (2 mM sodium orthovanadate, 2 mM molybdate and 2 mM sodium pyrophosphate) and protease inhibitors (2 mM benzamidine, 0.5 mM aprotinin and 1 mM phenylmethylsulphonyl fluoride). Each sample was centrifuged, and the supernatant was then boiled in sample buffer (1.5% dithiothreitol, 2% SDS, 80 mM Tris-HCl, pH 6.8, 10% glycerol and 0.01% bromphenol blue) for 5 min. Proteins were separated by SDS-PAGE and transferred to nitrocellulose. The nitrocellulose membrane was blocked with 2–5% milk or LiCor Odyssey blocking buffer (Li-Cor, Lincoln, NE, USA) for 1 h and probed with primary antibodies against proteins of interest overnight followed by secondary antibodies for 1 h. Proteins were visualized by enhanced chemiluminescence or by infrared fluorescence using an Odyssey imager (LiCor).

Transfection of SM tissues

S100A4 short hairpin RNA (shRNA) plasmids, S100A4 wild-type (WT) plasmids, RhoA shRNA plasmids or rhotekin small interfering RNA (siRNA) were introduced into tracheal SM strips by the method of reversible permeabilization (Tang & Gunst, 2001; Tang *et al.* 2003; Zhang *et al.* 2005; Zhang *et al.* 2012; Zhang *et al.* 2018). Tissues were equilibrated and muscles were lengthened until the isometric force was stable. Muscle strips were then attached to metal mounts to maintain them at constant length. The strips were incubated successively in each of the following solutions: *Solution 1* (at 4°C for 120 min) containing (in mM): 10 EGTA, 5 Na_2ATP, 120 KCl, 2 $MgCl_2$ and 20 *N*-tris (hydroxymethyl) methyl-2-aminoethanesulphonic acid (TES); *Solution 2* (at 4° C overnight) containing (in mM): 0.1 EGTA, 5 Na_2ATP, 120 KCl, 2 $MgCl_2$, 20 TES and 20 μg mL^{-1} S100A4 shRNA or RhoA shRNA plasmid or 10 μg mL^{-1} rhotekin siRNA. *Solution 3* (at 4° C for 30 min) containing (in mM): 0.1 EGTA, 5 Na_2ATP, 120 KCl, 10 $MgCl_2$ and 20 TES; and *Solution* 4 (at 22° C for 90 min) containing (in mM): 110 NaCl, 3.4 KCl, 0.8 $MgSO_4$, 25.8 $NaHCO_3$, 1.2

KH_2PO_4, and 5.6 dextrose. *Solutions 1–3* were maintained at pH 7.1 and aerated with 100% O_2. *Solution 4* was maintained at pH 7.4 and was aerated with 95% O_2–5% CO_2. After 30 min in *Solution 4*, $CaCl_2$ was added gradually to reach a final concentration of 2.4 mM. The strips were then incubated in a CO_2 incubator at 37°C for 2 days in serum-free Dulbecco's modified Eagle's medium containing 5 mM Na_2ATP, 100 U mL^{-1} penicillin, 100 μg mL^{-1} streptomycin, 50 μg mL^{-1} kanamycin, 2.5 μg mL^{-1} anti-fungal and 20 μg mL^{-1} S100A4 shRNA or WT S100A4 plasmids or 20 μg mL^{-1} RhoA shRNA plasmids or 10 μg mL^{-1} rhotekin siRNA to allow for expression of the recombinant proteins. The depletion of S100A4, RhoA or rhotekin proteins in transfected muscle tissues was confirmed by immunoblotting.

Cell dissociation

Freshly dissociated primary cells were used for these studies to avoid the morphological changes in cytoskeletal organization and the changes in phenotype that occur during the culture of SM cells. SM cells were enzymatically dissociated from tracheal muscle strips (Opazo Saez *et al*. 2004; Zhang *et al*. 2005). Tracheal muscle strips were minced and transferred to 5 mL of dissociation solution (in mM: 130 NaCl, 5 KCl, 1.0 $CaCl_2$, 1.0 $MgCl_2$, 10 Hepes, 0.25 EDTA, 10 D-glucose and 10 taurine, pH 7.0) with collagenase (type IV, 400 U mL^{-1}), papain (type IV, 30 U mL^{-1}), bovine serum albumin (1 mg mL^{-1}) and dithiothreitol (DTT) (1 mM). All enzymes were obtained from Sigma (St Louis, MO, USA). The strips were then placed in a 37°C shaking water bath at 60 oscillations min^{-1} for 15–20 min, followed by three washes with a Hepes-buffered saline solution (in mM: 130 NaCl, 5 KCl, 1.0 $CaCl_2$, 1.0 $MgCl_2$, 20 Hepes and 10 D-glucose, pH 7.4) and triturated with a pipette to liberate individual SM cells from the tissue. The solution containing the dissociated cells was poured over glass slides, and the cells were allowed to adhere to the slides for 30–60 min at 37°C. Cells were stimulated with 10^{-5} M ACh for 5 min at 37°C or left unstimulated. Stimulated and unstimulated cells were fixed for 10 min in 4% paraformaldehyde (v/v) in phosphate-buffered saline (in mM: 137 NaCl, 4.3 Na_2HPO_4, 1.4 KH_2PO_4 and 2.7 KCl, pH 7.4).

Primary cells dissociated from tracheal SM tissue strips after dissection from other tissue components consist almost entirely of SM cells and express high levels of SM the SM phenotype-specific protein, SM myosin heavy chain (Huang & Gunst, 2020). Immunofluorescence analysis shows that extracellular matrix proteins remain extensively bound to the cell surface after dissociation (Huang & Gunst, 2020). We have directly compared the effects of different stimuli on protein interactions and localization in isolated freshly dissociated cells and intact tissues using a proximity ligation assay (PLA) or immunofluorescence and have observed qualitatively similar results (Zhang *et al*. 2015; Huang & Gunst, 2020).

In situ PLA

In situ PLA was performed as described previously to detect interactions between proteins (Huang *et al*. 2011; Zhang *et al*. 2012, 2016; Zhang & Gunst, 2017). PLA provides for the precise detection of protein-protein complexes (Soderberg *et al*. 2006; Soderberg *et al*. 2008).

Target proteins are reacted with primary antibodies raised in different species, and a pair of oligonucleotide-labelled secondary antibodies conjugated to + and – PLA probes are targeted to each pair of primary antibodies. The probes form circular DNA strands only when they are bound in very close proximity (<40 nm). These DNA circles serve as templates for localized rolling circle amplification, generating a fluorescence signal (spot) that enables individual interacting pairs of the target protein molecules to be visualized. The PLA signal thus allows for the detection of a complexes between target proteins at a very high resolution.

SM cells were dissociated from sham-treated or transfected canine tracheal SM tissues. Freshly dissociated SM cells were stimulated with 10^{-5} M Ach or left unstimulated and then fixed, permeabilized and incubated with primary antibodies against target proteins or epitopes followed by a pair of oligonucleotide-labelled secondary antibodies conjugated to Duolink + and − PLA probes. PLA probe hybridization, ligation, amplification and detection media were administered in accordance with the manufacturer's instructions (Olink Bioscience, Uppsala, Sweden). Randomly selected cells from both unstimulated and ACh-stimulated groups were analysed for protein interactions by visualizing PLA fluorescence spots using a LSM 510 confocal microscope (Carl Zeiss, Oberkochen, Germany). The total number of PLA fluorescence spots per cell was counted using Image Tools (Olink Bioscience). For analysis of the cellular localization of complexes between vinculin and paxillin, the ratio of the pixel intensity between the submembranous area of the cell cytoplasm and rest of the cell cytoplasm was analysed using Metamorph (Molecular Devices, Inc., Sunnyvale, CA, USA) as described previously (Zhang *et al.* 2012; Zhang & Gunst, 2017) (see Supporting Information, Fig. 3).

Triton solubility assay

A Triton solubility assay was performed on extracts of SM tissues to separate cytoskeletal and Triton-soluble proteins (Dulyaninova *et al.* 2007; Li *et al.* 2010; Kiboku *et al.* 2013; Zhang & Gunst, 2017; Zhang *et al.* 2018). Frozen and pulverized tracheal SM tissue samples were mixed with Triton X-100 lysis buffer (150 mM KCl, 20 mM Pipes, 10 mM imidazole, pH 7.0, 0.05% Triton X-100, 1 mM $MgCl_2$, 1 mM EGTA, 1 mM DTT, 0.1 mM PMSF, 5 μg mL^{-1} aprotinin, 5 μg mL^{-1} leupeptin, 2 μg mL^{-1} pepstatin A, 1 mM Na_3VO_4 and 20 mM β-glycerophosphate) at 4°C. After 5 min, the lysates were centrifuged at 8,000 *g* for 5 min at 4°C and the supernatant was removed as the soluble fraction. The pellet, the insoluble fraction, was added to equal volumes of Triton X-100 lysis buffer with additional 0.8% SDS and 2 mM EDTA, boiled for 5 min and rotated for 1 h and then centrifuged at 16,000 *g* for 15 min at 4°C. The supernatant was transferred to another tube as the insoluble fraction. Equal volumes of soluble and insoluble fractions from the same sample were used to obtain for immunoblots of NM myosin IIA or NM myosin IIB. The ratio of each protein in the pellet fraction (cytoskeletal) *vs.* the soluble fraction (cytosolic) was calculated.

Analysis of F-actin and G-actin

The relative proportions of F-actin and G-actin in SM tissues were analysed as described previously (Zhang *et al.* 2005). Briefly, each of the tracheal SM strips was homogenized in 200 μL of F-actin stabilization buffer (50 mM Pipes, pH 6.9, 50 mM NaCl, 5 mM $MgCl_2$, 5

mM EGTA, 5% glycerol, 0.1% Triton X-100, 0.1% Nonidet P-40, 0.1% Tween-20, 0.1% β-mercaptoethanol, 0.001% anti-foam, 1 mM ATP, 1 μg mL^{-1} pepstatin, 1 μg mL^{-1} leupeptin, 10 μg mL^{-1} benzamidine and 500 μg mL^{-1} tosyl arginine methyl ester). Supernatants of the protein extracts were collected after centrifugation (Optima MAX Ultracentrifuge; Beckman Coulter, Brea, CA, USA) at 150 000 *g* for 60 min at 37° C. The pellets were resuspended in 150 μL of ice-cold water containing 10 μM cytochalasin D and then incubated on ice for 1 h to depolymerize F-actin. The resuspended pellets were mixed gently every 15 min. Four microlitres of supernatant (G-actin) and pellet (F-actin) fractions were subjected to immunoblot analysis using anti-actin antibody (clone AC-40; Sigma). The ratios of F-actin to G-actin were determined using densitometry.

Measurement of myosin RLC phosphorylation

Myosin light chain phosphorylation was analysed as described previously (Zhang *et al.* 2005; Zhang *et al.* 2012; Zhang & Gunst, 2017; Zhang *et al.* 2018). Frozen muscle strips were immersed in dry ice precooled in acetone containing 10% w/v trichloroacetic acid and 10 mM DTT. Proteins were extracted in 8 M urea, 20 mM Tris base, 22 mM glycine and 10 mM DTT. Phosphorylated and unphosphorylated myosin light chains were separated by glycerol–urea polyacrylamide gel electrophoresis, transferred to nitrocellulose then immunoblotted for myosin RLC. Myosin RLC phosphorylation was calculated as the ratio of phosphorylated myosin RLC to total RLC.

Reagents and antibodies

The sources of antibodies were as follows: monoclonal mouse anti-human RhoA (catalogue no. MA1134; Invitrogen, Carlsbad, CA, USA); polyclonal Rabbit anti-human S100A4 (catalogue no. PA532576; Invitrogen); polyclonal Rabbit anti-human Rhotekin (catalogue no. PA529931; Invitrogen); monoclonal mouse anti-human Rhotekin (catalogue no. MA526050, Invitrogen); polyclonal rabbit anti-human phospho-Ser1943 NM myosin II (catalogue no. 5026; Cell Signaling Technology, Beverly, MA, USA); polyclonal rabbit anti-human NM myosin IIA (catalogue no. M8064; Sigma); monoclonal mouse anti-human NM myosin IIA (catalogue no. MA527765; Invitrogen); polyclonal rabbit anti-human NM myosin IIB (catalogue no. M7939; Sigma); monoclonal mouse anti-human paxillin (catalogue no. 610 569; BD Transduction, San Jose, CA, USA); polyclonal rabbit anti-human paxillin phospho-tyrosine 118 (catalogue no. 44–722G; Invitrogen); monoclonal mouse anti-human vinculin (clone hVIN-1, v9131; Sigma); polyclonal rabbit anti-human vinculin phospho-tyrosine 1065 (catalogue no. 44–1078G; Invitrogen); horse-radish peroxidase-conjugated IgG (catalogue no. NA931 & NA934; Amersham Biosciences, Little Chalfont, UK); IRDye® 680RD Donkey-anti-Mouse IgG (catalogue no. 926–68 070; LiCor) and IRDye® 800CW Donkey-anti-Rabbit IgG (catalogue no. 925–32 211; LiCor); polyclonal rabbit anti-canine cardiac vinculin and polyclonal rabbit anti-bovine SM and NM myosin II regulatory light chain were custom made by BABCO (Richmond, CA, USA). All antibodies have been validated in previous studies by confirming their reaction with the designated antigen in the SM tissue extracts, immunoblots or fixed cells (Tang *et al.* 2003; Opazo Saez *et al.* 2004; Zhang *et al.* 2010; Huang *et al.* 2011; Zhang *et al.* 2012; Zhang & Gunst, 2017). Antibodies against S100A4 and rhotekin are validated in the present study.

The reagents for Duolink™ *in situ* PLA were obtained from Millipore Sigma (Burlington, MA, USA). Odyssey blocking buffer (catalogue no. 927–50 000) was obtained from LiCor Biosciences.

Rhotekin siRNA (catalogue no. SC-39 223) was purchased from Santa Cruz Biotechnology, Inc. (Dallas, TX, USA). S100A4 shRNA plasmids (catalogue no. TG309668), RhoA shRNA plasmids (catalogue no. TG309823) and pCMV6-XL4 human untagged S100A4 plasmids (catalogue no. SC109749) were purchased from OriGene Technologies, Inc. (Rockville, MD, USA). The *Escherichia coli* (Bluescript) transformed with these plasmids were grown in LB medium, and plasmids were purified by alkaline lysis with SDS using a purification kit from Qiagen Inc. (Valencia, CA, USA).

Statistical analysis

Comparisons between two groups were performed using a paired or unpaired two-tailed Student's *t* test, and comparisons among multiple groups were performed by ANOVA with or without repeated measures using Tukey's test for *post hoc* analysis. Details of the analysis of data are provided in the Supporting Information. Values of '*n*' refer to the number of individual cells or tissue strips used to obtain mean values. Sets of tissues or groups of cells for each experiment were obtained from different animals. $P < 0.05$ was considered statistically significant.

Results

S100A4 mediates myosin heavy chain assembly and tension development in airway SM tissues in response to contractile stimulation (Fig. 1)

The role of S100A4 in the regulation of contractile tension development and NM myosin II filament assembly in airway SM was evaluated by using shRNA to deplete tissues of S100A4 and by transfecting tracheal muscle tissues with WT S100A4 to increase expression. Treatment of airway SM tissues with shRNA for S100A4 resulted in the depletion of S100A4 to 35.6 ± 10.8% of sham-treated tissues (Fig. 1A) and reduced tension development in response to 5 min 10^{-5} M ACh to 56.3 ± 1.9% of sham-treated tissues (Fig. 1B). The transfection of tissues with WT S100A4 increased protein expression by 59.2 ± 11.1%, but it had no significant effect on tension development.

The effect of S100A4 depletion on the polymerization of NM myosin IIA and IIB in response to stimulation with 10^{-5} M ACh was assessed by measuring the ratio of each NM myosin II isoform in the Triton X-insoluble (cytoskeletal) *vs.* Triton X-soluble (cytosolic) fractions of tracheal tissue extracts as described previously (Li & Bresnick, 2006; Li *et al.* 2010; Zhang & Gunst, 2017; Zhang *et al.* 2018) (Fig. 1C). In tissues subjected to sham transfections, the ratios of both NM myosin IIA and NM myosin IIB in the cytoskeletal/soluble fractions increased significantly in response to 5 min of stimulation with ACh, whereas the depletion of S100A4 inhibited the increase in ratios of NM myosin IIA and NM myosin IIB in the cytoskeletal/soluble fractions in ACh-stimulated tissues. These results demonstrate that S100A4 depletion inhibits NM myosin filament assembly in tracheal SM tissues.

In situ PLA analysis was also used to assess NM myosin II filament formation during contractile stimulation of freshly dissociated tracheal SM cells (Fig. 1D). Monomers of NM myosin IIA and IIB isoforms can coassemble into heterotypic filaments (Beach *et al*. 2014; Beach & Hammer, 2015; Zhang & Gunst, 2017); therefore, interactions between NM myosin IIA and IIB isoforms can be quantified to assess the formation of NM myosin II polymers (Zhang & Gunst, 2017; Zhang *et al*. 2018) (Fig. 1D). SM cells were dissociated from S100A4-depleted tissues and from sham-treated tissues. In cells from sham-treated tissues, ACh stimulation induced interactions between NM myosin IIA and IIB isoforms, indicating NM myosin filament formation. By contrast, few interactions between NM myosin IIA and IIB isoforms were observed in cells from S100A4-depleted tissues. These observations provide further evidence that S100A4 regulates NM myosin filament assembly in SM tissues stimulated by ACh.

NM myosin IIA undergoes phosphorylation on Ser 1943 on the non-helical terminal tail domain of its heavy chain in response to contractile stimulation in airway SM and this phosphorylation is required for NM myosin filament assembly (Zhang & Gunst, 2017). We evaluated the effect of depleting S100A4 on ACh-induced NM myosin II heavy chain Ser 1943 phosphorylation in tracheal SM tissues. The depletion of S100A4 prevented the increase in NM myosin II heavy chain Ser1943 phosphorylation in response to ACh stimulation (Fig. 1E).

All of these results support the conclusion that S100A4 plays a critical role in regulating the polymerization of NM myosin II filaments in airway SM in response to contractile stimulation.

Contractile stimulation induces the formation of a complex between S100A4 and NM myosin II in airway SM (Fig. 2)

We evaluated the effect of stimulation with ACh on the interaction between S100A4 and NM myosin II in tracheal SM tissues. S100A4 was immunoprecipitated from tracheal SM tissue extracts and immunocomplexes were blotted for S100A4 and NM myosin IIA or IIB isoforms (Fig. 2A). Stimulation of tracheal SM tissues for 5 min with 10^{-5} M ACh increased the coprecipitation of both NM myosin IIA and NM myosin IIB with S100A4 in tracheal SM tissues.

We also used *in situ* PLA analysis to assess interactions between NM myosin II isoforms and S100A4 in freshly dissociated tracheal SM cells (Fig. 2B). We observed few interactions between either NM myosin II isoform and S100A4 in unstimulated cells, although the interaction of both NM myosin IIA and IIB isoforms with S100A4 dramatically increased in cells stimulated with ACh. Interactions between NM myosin isoforms and S100A4 were localized to the cortical region of the SM cells (Fig. 2B). We also used PLA to probe for interactions between S100A4 and SM myosin II. As expected, almost no interactions between S100A4 and SM myosin II were detected in unstimulated or ACh-stimulated SM cells (Fig. 2C).

These results demonstrate that contractile stimulation triggers the interaction between S100A4 and NM myosin IIA and IIB isoforms in the cortical region of airway SM cells. *In*

vitro protein studies have indicated that S100A4 binds preferentially to the NM myosin IIA isoform (Li & Bresnick, 2006; Kiss *et al.* 2012; Ramagopal *et al.* 2013). By contrast, our results suggest that S100A4 may bind to both A and B isoforms of NM myosin II *in vivo*. However, because NM myosin IIA and IIB can assemble into heterotypic filaments, it is possible that S100A4 binds preferentially to one NM myosin isoform and that the interaction with the other isoform is indirect.

In sum, these results demonstrate that ACh stimulates the formation of a complex between S100A4 and NM myosin II in airway SM.

S100A4 is required for the assembly and activation of membrane adhesion junction signalling complexes (adhesomes) in response to contractile stimulation (Fig. 3)

In airway SM, NM myosin II provides the motor for the recruitment of adhesome proteins to the membrane in response to contractile stimulation. The polymerization of NM myosin at the cortex of the SM cell is required for adhesome complex assembly and activation (Zhang & Gunst, 2017).

Vinculin and paxillin are binding partners and form a complex that is stably maintained in both unstimulated and stimulated airway SM tissues (Opazo Saez *et al.* 2004; Huang *et al.* 2011; Zhang *et al.* 2012). In unstimulated muscle cells, inactive vinculin/paxillin complexes are distributed throughout the cytoplasm. The stimulation of tracheal SM tissues and cells with ACh causes vinculin/paxillin complexes to be recruited to membrane adhesion junctions (Opazo Saez *et al.* 2004; Huang *et al.* 2011; Zhang *et al.* 2012). After localization to membrane adhesome complexes, vinculin undergoes phosphorylation on Tyr1065 at its C-terminus, which promotes a conformational change that enables it to bind to talin and F-actin (Huang *et al.* 2011; Huang *et al.* 2014). Paxillin undergoes phosphorylation on Tyr31 and Tyr118 after localization to adhesome complexes, regulating its coupling to signalling modules that catalyse actin polymerization (Tang *et al.* 2003; Tang *et al.* 2005; Huang *et al.* 2011; Zhang *et al.* 2012, 2016; Zhang & Gunst, 2017; Zhang *et al.* 2018; Huang & Gunst, 2020).

We used PLA to determine whether S100A4 is required for the localization of paxillin/vinculin complexes to membrane adhesomes and for the interaction of vinculin with talin during contractile stimulation with ACh (Fig. 3A and B). In sham-treated cells, ACh stimulated the localization of vinculin/paxillin complexes along the membrane and ACh also induced an increase in the interaction of vinculin and talin. The depletion of S100A4 prevented both the ACh-induced recruitment of paxillin/vinculin complexes to the membrane, as well as the interaction between vinculin and talin (Fig. 3A and B). We also analysed the effect of depleting S100A4 on the tyrosine phosphorylation of both paxillin and vinculin in response to contractile stimulation with ACh (Fig. 3C). The increases in vinculin Tyr1065 phosphorylation and paxillin Tyr118 phosphorylation induced by ACh were both inhibited by the depletion of S100A4.

The effect of depleting S100A4 on actin polymerization in response to ACh was evaluated using a fractionation assay to separate soluble (G-actin) and insoluble (F-actin) actin in the

muscle extracts (Fig. 3D). Depletion of S100A4 inhibited the increase in actin polymerization that occurs in response to stimulation with ACh.

The role of S100A4 with respect to regulating the phosphorylation of the RLC of SM and NM myosin II was also analysed in extracts of muscle tissues stimulated with ACh (Fig. 3E). NM myosin RLC comprises 20% of the total myosin RLC in airway SM tissues (Zhang & Gunst, 2017); however, NM and SM myosin RLC isoforms cannot be distinguished immunologically because their sequences differ only slightly (Gaylinn *et al*. 1989; Yuen *et al*. 2009). The depletion of S100A4 had no significant effect on the phosphorylation of myosin RLC induced by stimulation with ACh (Fig. 3E).

These results suggest that S100A4 contributes to the contractile activation of airway SM by regulating the assembly of NM myosin filaments, which in turn mediate the formation and activation of adhesome signalling complexes at the cell membrane. The activation of signalling modules within membrane adhesomes is necessary to catalyse actin polymerization in response to contractile stimulation. However, the phosphorylation of myosin RLC is catalysed by pathways that are independent of adhesome signalling and thus unaffected by the depletion of S100A4.

RhoA regulates the interaction of S100A4 with NM myosin IIA during contractile stimulation (Fig. 4)

RhoA inactivation inhibits NM myosin filament assembly in response to contractile stimulation in airway SM (Zhang & Gunst, 2017). We hypothesized that RhoA might regulate NM myosin filament assembly by regulating the interaction between S100A4 and NM myosin II.

We evaluated the effect of contractile stimulation on the formation of complexes between RhoA, S100A4 and NM myosin II by immunoprecipitating RhoA or S100A4 from extracts of unstimulated and ACh-stimulated tracheal muscle tissues. ACh stimulation significantly increased the formation of complexes between RhoA, S100A4 and NM myosin II (Fig. 4A). In ACh-stimulated muscles, the amounts of S100A4 and NM myosin II were significantly higher in RhoA immunoprecipitates; conversely, the amount of RhoA was increased in S100A4 immunoprecipitates. These results demonstrate that ACh stimulation induces the interaction of RhoA with S100A4 and NM myosin IIA.

The effects of contractile stimulation on the interactions of RhoA with S100A4 and NM myosin II were also assessed using *in situ* PLA analysis in freshly dissociated tracheal SM cells (Fig. 4B). There were few interactions between RhoA and NM myosin IIA or RhoA and S100A4 in unstimulated SM cells, but the interactions between RhoA and NM myosin IIA were dramatically increased in cells stimulated with ACh.

RhoA was depleted from airway SM tissues using RhoA shRNA (Fig. 4C). Treatment of the tissues with RhoA shRNA inhibited the ACh-induced contractile force. *In situ* PLA analysis was used to assess the effect of RhoA depletion on the interaction between S100A4 and NM myosin IIA in freshly dissociated tracheal SM cells. The depletion of RhoA GTPase inhibited the interaction of S100A4 and NM myosin in response to contractile stimulation

with ACh (Fig. 4D). The role of S100A4 in the interaction between RhoA and NM myosin IIA was also evaluated in cells depleted of S100A4. The ACh-induced interaction of RhoA and NM myosin was inhibited in cells from S100A4-depleted tissues (Fig. 4E).

These results suggest that RhoA regulates NM myosin filament assembly during contractile stimulation by regulating the interaction of S100A4 with NM myosin II.

Rhotekin couples RhoA to S100A4 and mediates the activation of NM myosin filament assembly (Fig. 5)

S100A4 has been shown to bind to rhotekin, which specifically binds only to activated RhoA, RhoA GTP (Chen *et al.* 2013). We hypothesized that RhoA might regulate S100A4 binding to NM myosin II via rhotekin.

The effect of contractile stimulation on the interaction of rhotekin with S100A4, NM myosin II and activated RhoA was evaluated by immunoprecipitating rhotekin from extracts of unstimulated and ACh-stimulated tissues. ACh stimulation significantly increased the coprecipitation of RhoA, S100A4 and NM myosin II with rhotekin, indicating that ACh stimulation induces the formation of a protein complex between RhoA, rhotekin, S100A4 and NM myosin IIA (Fig. 5A).

The effects of contractile stimulation on the interaction between rhotekin and RhoA, S100A4 and NM myosin II were also assessed using *in situ* PLA analysis in freshly dissociated tracheal SM cells (Fig. 5B). There were few interactions between rhotekin and RhoA, S100A4 or NM myosin II in unstimulated SM cells, but the interactions between rhotekin and RhoA, S100A4 or NM myosin IIA were dramatically increased in cells stimulated with ACh. These results support our hypothesis that rhotekin mediates the interaction of activated RhoA with S100A4 and NM myosin.

Rhotekin was depleted from SM tissues using rhotekin siRNA and the effect on the association between RhoA and S100A4 was determined (Fig. 5C and D). The depletion of rhotekin inhibited the interaction of RhoA with S100A4 in response to stimulation with ACh, demonstrating that rhotekin mediates the interaction of activated RhoA with S100A4 and NM myosin IIA (Fig. 5D).

The role of rhotekin in NM myosin II assembly was analysed using the Triton X-soluble fractionation assay and by measuring the interaction between NM myosin IIA and IIB isoforms using PLA (Fig. 6A and B). The depletion of rhotekin inhibited the ACh-induced increase in NM myosin filament formation as measured by both assays. Rhotekin depletion also prevented the increase in serine 1943 phosphorylation on NM myosin II in response to ACh, which is required for NM myosin filament assembly (Fig. 6C).

We further assessed the effect of rhotekin depletion the interaction of vinculin with talin in response to ACh. The ACh-induced increase in the interaction between vinculin and talin was completely inhibited in cells dissociated from rhotekin-depleted tissues (Fig. 6D). The increases in vinculin Tyr1065 phosphorylation and paxillin Tyr118 phosphorylation induced by ACh were also inhibited by the depletion of rhotekin (Fig. 6E).

These results support our hypothesis that Ach regulates the assembly of NM myosin into filaments by activating RhoA, which regulates the interaction of S100A4 with NM myosin II by coupling to rhotekin.

Discussion

S100A4 is widely expressed in a variety of cell and tissue types; however, little is known about its physiologic function in normal cells and tissues. The results of the present study demonstrate that S100A4 plays a key role in the process of contraction and tension generation in airway SM tissues by regulating the assembly of NM myosin II into filaments that catalyse the recruitment of cytoskeletal proteins to adhesome signalling complexes (Fig. 7). We found that the contractile stimulation of airway SM triggers the coupling of S100A4 to NM myosin II at the cortex of the cell, and that S100A4 is critical for the assembly of NM myosin II into filaments. The depletion of S100A4 from airway SM tissues inhibits NM myosin filament polymerization in response to contractile stimulation, consequently preventing the recruitment of vinculin and paxillin to adhesome complexes. This inhibits actin polymerization and tension development (Figs 1–3).

We also found that the coupling of S100A4 to NM myosin II is directly regulated by RhoA GTPase (Fig. 4). The coupling of S100A4 to NM myosin by activated RhoA is mediated by the RhoA-binding protein, rhotekin (Figs 4 and 5). Rhotekin selectively interacts with activated GTP-bound RhoA, and it can also bind to S100A4 within its Rho-binding domain (Reid *et al.* 1996; Chen *et al.* 2013). Thus, the activation of RhoA in response to ACh leads to the formation of a complex between activated RhoA, rhotekin, S100A4 and NM myosin II. S100A4 binds to the NM myosin IIA heavy chain near the C-terminal end of its coiled-coil domain (Li & Bresnick, 2006; Malashkevich *et al.* 2008; Kiss *et al.* 2012; Ramagopal *et al.* 2013); thus, RhoA regulates NM myosin polymerization in airway SM by regulating the binding of S100A4 to the heavy chain of NM myosin II. Consistent with these observations, we previously found that RhoA activation is required for NM myosin filament polymerization, and that RhoA also regulates the phosphorylation NM myosin heavy chain on Ser1943, which is required for NM myosin II assembly in airway SM tissues (Zhang & Gunst, 2017).

Contractile stimulation induces the phosphorylation of the RLCs of both SM and NM myosin II (Vicente-Manzanares *et al.* 2009; Zhang *et al.* 2010; Zhang & Gunst, 2017). In airway SM, RhoA regulates NM myosin RLC phosphorylation but not SM RLC phosphorylation during contractile stimulation with ACh (Zhang *et al.* 2010; Zhang *et al.* 2012; Zhang & Gunst, 2017). Studies of the molecular function of myosin RLC phosphorylation suggest that RLC phosphorylation can regulate both NM and SM myosin II filament assembly by converting myosin monomers from a folded assembly-incompetent state to an open ‘assembly-competent’ state capable of filament formation (Craig *et al.* 1983; Trybus & Lowey, 1987; Citi *et al.* 1989; Kiboku *et al.* 2013). In the present study, the depletion of S100A4 prevented myosin filament assembly without affecting total (NM and SM) myosin RLC phosphorylation in response to ACh (Fig. 3E). This suggests that the RhoA-mediated interaction of S100A4 with myosin heavy chain regulates NM myosin II assembly in response to ACh. However, it does not rule out the possibility that RhoA may

also catalyse a change in the conformation of NM myosin II monomers through its effects on NM myosin RLC phosphorylation, or that RhoA may also regulate the activation of cross-bridge cycling by NM myosin. Thus, RhoA may regulate both the assembly and activation of NM myosin in airway SM through distinct effects on the NM myosin heavy chain and regulatory light chains.

Previous studies of the molecular interaction of S100A4 with NM myosin have concluded that the binding of S100A4 to NM myosin II filaments promotes filament depolymerization (Li *et al*. 2003; Li & Bresnick, 2006; Malashkevich *et al*. 2008; Kiss *et al*. 2012). Biochemical analysis of interactions between S100A4 and myosin IIA rods *in vitro* showed that S100A4 inhibited the assembly of myosin IIA monomers into filaments and promoted the disassembly on myosin IIA filaments into monomers (Li *et al*. 2003; Li & Bresnick, 2006). S100A4 binds to the C-terminal end of the coiled-coil domain of NM myosin IIA, overlapping the assembly-competent domain that is required for filament formation. Structural models of the interaction of S100A4 with the heavy chain of NM myosin II have led to proposals regarding the molecular mechanism by which S100A4 promotes myosin filament disassembly (Kiss *et al*. 2012). Thus, the results of the present study conducted in airway SM tissues appear to conflict with previous conclusions regarding the molecular function of S100A4.

Our conclusion that S100A4 promotes the assembly of NM myosin filaments rather than myosin filament disassembly is supported by multiple approaches to assess NM myosin filament assembly: (i) The depletion of S100A4 from airway SM inhibited the ACh-induced increase in the proportion of NM myosin II in the cytoskeletal *vs*. Triton-soluble fractions of SM tissue extracts, which has been previously used to assess myosin polymerization in multiple cell types (Dulyaninova *et al*. 2007; Li *et al*. 2010; Kiboku *et al*. 2013; Zhang & Gunst, 2017; Zhang *et al*. 2018). (ii) The depletion of S100A4 also inhibited the interaction between NM myosin IIA and NM myosin IIB isoforms in response to ACh, which we previously demonstrated to be a reliable index of myosin polymerization (Zhang & Gunst, 2017). (iii) The depletion of S100A4 inhibited the ACh-induced phosphorylation of NM myosin on Ser1943 in airway SM tissues, which is required for NM myosin filament assembly in this tissue. Furthermore, we found that the depletion of S100A4 from airway SM tissues inhibits the assembly and activation of adhesome complexes, which is dependent on NM myosin II polymerization (Zhang & Gunst, 2017). Thus, we must conclude that the physiologic function of S100A4 in airway SM tissues differs from that previously proposed based on molecular studies *in vitro*.

The differences regarding the role of S100A4 found in our studies performed in living cells and tissues *vs*. those from *in vitro* biochemical studies could reflect differences in the experimental conditions. In the molecular studies *in vitro*, only the rod domain of the NM myosin II molecule was used, which may not be a reliable replacement for the full-length NM myosin II molecule. In addition, myosin-binding regulatory proteins and the cytoplasmic milieu present in *vivo* may affect the interactions of S100A4 with NM myosin or the effects of S100A4 on NM myosin function. It is also possible that NM myosin II filament assembly in living cells initially requires the disassembly of existing NM myosin II

filaments to generate a pool of monomers that are reincorporated into *de novo* NM myosin II filaments.

The function of S100A4 may also differ among cell types in which NM myosin II plays distinct and cell-specific roles. The cellular function of NM myosin is quite different in SM than in motile NM cells such as macrophages. In SM cells, NM myosin constitutes a small subset of the total myosin in the cell (20%) (Zhang & Gunst, 2017), whereas the motility of macrophages and other crawling cells is entirely dependent on NM myosin II assembly and its activation. NM myosin is not the primary motor protein for shortening and tension generation in SM; rather, it serves in a subsidiary role to regulate the organization and assembly of cytoskeletal signalling complexes. Thus, the cellular function of S100A4 might vary in different cell types as a reflection of cell-specific differences in the physiologic function of NM muscle myosin II.

In addition to its intracellular functions, S100A4 can secreted or released from cells and can act extracellularly in an autocrine or paracrine fashion to regulate the phenotype and functions of target cells (Ambartsumian *et al.* 2019). S100A4 has been reported in the extracellular fluids of subjects with several inflammatory diseases, including asthma and seasonal allergic rhinitis, rheumatoid arthritis and allergic dermatitis (Klingelhofer *et al.* 2007; Oslejskova *et al.* 2008; Bruhn *et al.* 2014; Ambartsumian *et al.* 2019). S100A4 is secreted extracellularly from airway SM tissues, and its secretion can be stimulated by inflammatory mediators such as interleukin-13 and tumour necrosis factor α (Wu *et al.* 2020). Extracellular S100A4 activates RAGE receptors on the airway SM cell surface to increase the endogenous expression of S100A4 and to stimulate inflammatory responses by airway SM tissues (Wu *et al.* 2020). Stimulation by inflammatory mediators triggers the recruitment and activation of signalling modules to adhesomes that are required for the regulation of airway SM phenotype and inflammatory responses (Zhang *et al.* 2007; Wu *et al.* 2008; Desai *et al.* 2011; Wu *et al.* 2016; Huang & Gunst, 2020). Thus, the activation of NM myosin by S100A4 may also play an important role in the assembly of adhesome signalling modules that mediate transitions in phenotype and a range of physiologic functions of airway SM.

Because S100A4 is ubiquitously expressed, it may play an essential role in regulating the physiologic functions of many cell types. Furthermore, its intracellular expression is up-regulated by a number of pathological conditions (Garrett *et al.* 2006; Ambartsumian *et al.* 2019). Thus, the mechanisms for the molecular function of S100A4 with respect to regulating NM myosin activity in airway SM may be broadly germane to its physiologic functions in other cells and tissues.

Supplementary Material

Refer to Web version on PubMed Central for supplementary material.

Acknowledgments

Funding

This work was supported by National Heart, Lung and Blood Institute Grants HL029289 and HL109629.

Biography

Wenwu Zhang trained as a cardiothoracic surgeon in China. He moved to Indianapolis, IN, USA in 2000 and obtained his PhD in Physiology from Indiana University in 2004. He joined the laboratory of Dr Susan Gunst at Indiana University School of Medicine, where he pursues research directed at the mechanisms by which cytoskeletal proteins regulate smooth muscle contractility and phenotypic expression in response to physiologic stimuli or changes in environmental conditions. His studies have described novel mechanisms by which adhesion junction signalling complexes regulate actin polymerization and the dynamics of cytoskeletal organization to regulate the responses of smooth muscle to a variety of physiologic stimuli.

References

Ambartsumian N, Klingelhofer J & Grigorian M (2019). The multifaceted S100A4 protein in cancer and inflammation. Methods Mol Biol 1929, 339–365. [PubMed: 30710284]

Beach JR & Hammer JA 3rd, (2015). Myosin II isoform co-assembly and differential regulation in mammalian systems. Exp Cell Res 334, 2–9. [PubMed: 25655283]

Beach JR, Shao L, Remmert K, Li D, Betzig E & Hammer JA 3rd, (2014). Nonmuscle myosin II isoforms coassemble in living cells. Curr Biol 24, 1160–1166. [PubMed: 24814144]

Boye K & Maelandsmo GM (2010). S100A4 and metastasis: a small actor playing many roles. Am J Pathol 176, 528–535. [PubMed: 20019188]

Bresnick AR (1999). Molecular mechanisms of nonmuscle myosin-II regulation. Curr Opin Cell Biol 11, 26–33. [PubMed: 10047526]

Brisset AC, Hao H, Camenzind E, Bacchetta M, Geinoz A, Sanchez JC, Chaponnier C, Gabbiani G & Bochaton-Piallat ML (2007). Intimal smooth muscle cells of porcine and human coronary artery express S100A4, a marker of the rhomboid phenotype in vitro. Circ Res 100, 1055–1062. [PubMed: 17347479]

Bruhn S, Fang Y, Barrenas F, Gustafsson M, Zhang H, Konstantinell A, Kronke A, Sonnichsen B, Bresnick A, Dulyaninova N, Wang H, Zhao Y, Klingelhofer J, Ambartsumian N, Beck MK, Nestor C, Bona E, Xiang Z & Benson M (2014). A generally applicable translational strategy identifies S100A4 as a candidate gene in allergy. Sci Transl Med 6, 214–218.

Chen M, Bresnick AR & O'Connor KL (2013). Coupling S100A4 to Rhotekin alters Rho signaling output in breast cancer cells. Oncogene 32, 3754–3764. [PubMed: 22964635]

Citi S, Cross RA, Bagshaw CR & Kendrick-Jones J (1989). Parallel modulation of brush border myosin conformation and enzyme activity induced by monoclonal antibodies. J Cell Biol 109, 549–556. [PubMed: 2474552]

Craig R, Smith R & Kendrick-Jones J (1983). Light-chain phosphorylation controls the conformation of vertebrate non-muscle and smooth muscle myosin molecules. Nature 302, 436–439. [PubMed: 6687627]

Davies BR, O'Donnell M, Durkan GC, Rudland PS, Barraclough R, Neal DE & Mellon JK (2002). Expression of S100A4 protein is associated with metastasis and reduced survival in human bladder cancer. J Pathol 196, 292–299. [PubMed: 11857492]

Desai LP, Wu YD, Tepper RS & Gunst SJ (2011). Mechanical stimuli and IL-13 interact at integrin adhesion complexes to regulate expression of smooth muscle myosin heavy chain in airway smooth muscle tissue. Am J Physiol Lung Cell Mol Physiol 301, L275–L284. [PubMed: 21642449]

Donato R, Cannon BR, Sorci G, Riuzzi F, Hsu K, Weber DJ & Geczy CL (2013). Functions of S100 proteins. Curr Mol Med 13, 24–57. [PubMed: 22834835]

Dulyaninova NG, House RP, Betapudi V & Bresnick AR (2007). Myosin-IIA heavy-chain phosphorylation regulates the motility of MDA-MB-231 carcinoma cells. Mol Biol Cell 18, 3144–3155. [PubMed: 17567956]

Eddinger TJ & Meer DP (2007). Myosin II isoforms in smooth muscle: heterogeneity and function. Am J Physiol Cell Physiol 293, C493–C508. [PubMed: 17475667]

Garrett SC, Varney KM, Weber DJ & Bresnick AR (2006). S100A4, a mediator of metastasis. J Biol Chem 281, 677–680. [PubMed: 16243835]

Gaylinn BD, Eddinger TJ, Martino PA, Monical PL, Hunt DF & Murphy RA (1989). Expression of nonmuscle myosin heavy and light chains in smooth muscle. Am J Physiol 257, C997–1004. [PubMed: 2531982]

Gross SR, Sin CG, Barraclough R & Rudland PS (2014). Joining S100 proteins and migration: for better or for worse, in sickness and in health. Cell Mol Life Sci 71, 1551–1579. [PubMed: 23811936]

Gunst SJ & Zhang W (2008). Actin cytoskeletal dynamics in smooth muscle: a new paradigm for the regulation of smooth muscle contraction. Am J Physiol Cell Physiol 295, C576–C587. [PubMed: 18596210]

Heissler SM & Sellers JR (2016). Various themes of myosin regulation. J Mol Biol 428, 1927–1946. [PubMed: 26827725]

Helfman DM, Kim EJ, Lukanidin E & Grigorian M (2005). The metastasis associated protein S100A4: role in tumour progression and metastasis. Br J Cancer 92, 1955–1958. [PubMed: 15900299]

Huang Y, Day RN & Gunst SJ (2014). Vinculin phosphorylation at Tyr1065 regulates vinculin conformation and tension development in airway smooth muscle tissues. J Biol Chem 289, 3677–3688. [PubMed: 24338477]

Huang Y & Gunst SJ (2020). Phenotype transitions induced by mechanical stimuli in airway smooth muscle are regulated by differential interactions of parvin isoforms with paxillin and Akt. Am J Physiol Lung Cell Mol Physiol 318, L1036–L1055. [PubMed: 32130030]

Huang Y, Zhang W & Gunst SJ (2011). Activation of vinculin induced by cholinergic stimulation regulates contraction of tracheal smooth muscle tissue. J Biol Chem 286, 3630–3644. [PubMed: 21071443]

Kiboku T, Katoh T, Nakamura A, Kitamura A, Kinjo M, Murakami Y & Takahashi M (2013). Nonmuscle myosin II folds into a 10S form via two portions of tail for dynamic subcellular localization. Genes Cells 18, 90–109. [PubMed: 23237600]

Kiss B, Duelli A, Radnai L, Kekesi KA, Katona G & Nyitray L (2012). Crystal structure of the S100A4-nonmuscle myosin IIA tail fragment complex reveals an asymmetric target binding mechanism. Proc Natl Acad Sci U S A 109, 6048–6053. [PubMed: 22460785]

Klingelhofer J, Senolt L, Baslund B, Nielsen GH, Skibshoj I, Pavelka K, Neidhart M, Gay S, Ambartsumian N, Hansen BS, Petersen J, Lukanidin E & Grigorian M (2007). Up-regulation of metastasis-promoting S100A4 (Mts-1) in rheumatoid arthritis: putative involvement in the pathogenesis of rheumatoid arthritis. Arthritis Rheum 56, 779–789. [PubMed: 17328050]

Lawrie A, Spiekerkoetter E, Martinez EC, Ambartsumian N, Sheward WJ, MacLean MR, Harmar AJ, Schmidt AM, Lukanidin E & Rabinovitch M (2005). Interdependent serotonin transporter and receptor pathways regulate S100A4/Mts1, a gene associated with pulmonary vascular disease. Circ Res 97, 227–235. [PubMed: 16002749]

Li ZH & Bresnick AR (2006). The S100A4 metastasis factor regulates cellular motility via a direct interaction with myosin-IIA. Cancer Res 66, 5173–5180. [PubMed: 16707441]

Li ZH, Dulyaninova NG, House RP, Almo SC & Bresnick AR (2010). S100A4 regulates macrophage chemotaxis. Mol Biol Cell 21, 2598–2610. [PubMed: 20519440]

Li ZH, Spektor A, Varlamova O & Bresnick AR (2003). Mts1 regulates the assembly of nonmuscle myosin-IIA. Biochemistry 42, 14258–14266. [PubMed: 14640694]

Lofgren M, Ekblad E, Morano I & Arner A (2003). Nonmuscle myosin motor of smooth muscle. J Gen Physiol 121, 301–310. [PubMed: 12668734]

Malashkevich VN, Varney KM, Garrett SC, Wilder PT, Knight D, Charpentier TH, Ramagopal UA, Almo SC, Weber DJ & Bresnick AR (2008). Structure of Ca^{2+}-bound S100A4 and its interaction with peptides derived from nonmuscle myosin-IIA. Biochemistry 47, 5111–5126. [PubMed: 18410126]

Opazo Saez A, Zhang W, Wu Y, Turner CE, Tang DD & Gunst SJ (2004). Tension development during contractile stimulation of smooth muscle requires recruitment of paxillin and vinculin to the membrane. Am J Physiol Cell Physiol 286, C433–C447. [PubMed: 14576084]

Oslejskova L, Grigorian M, Gay S, Neidhart M & Senolt L (2008). The metastasis associated protein S100A4: a potential novel link to inflammation and consequent aggressive behaviour of rheumatoid arthritis synovial fibroblasts. Ann Rheum Dis 67, 1499–1504. [PubMed: 18056757]

Ramagopal UA, Dulyaninova NG, Varney KM, Wilder PT, Nallamsetty S, Brenowitz M, Weber DJ, Almo SC & Bresnick AR (2013). Structure of the S100A4/myosin-IIA complex. BMC Struct Biol 13, 31. [PubMed: 24252706]

Reid T, Furuyashiki T, Ishizaki T, Watanabe G, Watanabe N, Fujisawa K, Morii N, Madaule P & Narumiya S (1996). Rhotekin, a new putative target for Rho bearing homology to a serine/threonine kinase, PKN, and rhophilin in the rho-binding domain. J Biol Chem 271, 13556–13560. [PubMed: 8662891]

Reimann S, Fink L, Wilhelm J, Hoffmann J, Bednorz M, Seimetz M, Dessureault I, Troesser R, Ghanim B, Klepetko W, Seeger W, Weissmann N & Kwapiszewska G (2015). Increased S100A4 expression in the vasculature of human COPD lungs and murine model of smoke-induced emphysema. Respir Res 16, 127. [PubMed: 26483185]

Soderberg O, Gullberg M, Jarvius M, Ridderstrale K, Leuchowius KJ, Jarvius J, Wester K, Hydbring P, Bahram F, Larsson LG & Landegren U (2006). Direct observation of individual endogenous protein complexes in situ by proximity ligation. Nat Methods 3, 995–1000. [PubMed: 17072308]

Soderberg O, Leuchowius KJ, Gullberg M, Jarvius M, Weibrecht I, Larsson LG & Landegren U (2008). Characterizing proteins and their interactions in cells and tissues using the in situ proximity ligation assay. Methods 45, 227–232. [PubMed: 18620061]

Tang DD & Gunst SJ (2001). Depletion of focal adhesion kinase by antisense depresses contractile activation of smooth muscle. Am J Physiol Cell Physiol 280, C874–C883. [PubMed: 11245605]

Tang DD, Turner CE & Gunst SJ (2003). Expression of non-phosphorylatable paxillin mutants in canine tracheal smooth muscle inhibits tension development. J Physiol 553, 21–35. [PubMed: 12949231]

Tang DD, Zhang W & Gunst SJ (2005). The adapter protein CrkII regulates neuronal Wiskott-Aldrich syndrome protein, actin polymerization, and tension development during contractile stimulation of smooth muscle. J Biol Chem 280, 23380–23389. [PubMed: 15834156]

Trybus KM & Lowey S (1987). Assembly of smooth muscle myosin minifilaments: effects of phosphorylation and nucleotide binding. J Cell Biol 105, 3007–3019. [PubMed: 2826495]

Vicente-Manzanares M, Ma X, Adelstein RS & Horwitz AR (2009). Non-muscle myosin II takes centre stage in cell adhesion and migration. Nat Rev Mol Cell Biol 10, 778–790. [PubMed: 19851336]

Wu Y, Huang Y & Gunst SJ (2016). Focal adhesion kinase (FAK) and mechanical stimulation negatively regulate the transition of airway smooth muscle tissues to a synthetic phenotype. Am J Physiol Lung Cell Mol Physiol 311, L893–L902. [PubMed: 27612967]

Wu Y, Huang Y, Herring BP & Gunst SJ (2008). Integrin-linked kinase regulates smooth muscle differentiation marker gene expression in airway tissue. Am J Physiol Lung Cell Mol Physiol 295, L988–997. [PubMed: 18805960]

Wu Y, Zhang W & Gunst SJ (2020). S100A4 is secreted by airway smooth muscle tissues and activates inflammatory signaling pathways via receptors for advanced glycation end products (RAGE). Am J Physiol Lung Cell Mol Physiol 319, L185–L195. [PubMed: 32432920]

Yuen SL, Ogut O & Brozovich FV (2009). Nonmuscle myosin is regulated during smooth muscle contraction. Am J Physiol Heart Circ Physiol 297, H191–H199. [PubMed: 19429828]

Zhang W, Bhetwal BP & Gunst SJ (2018). Rho kinase collaborates with p21-activated kinase to regulate actin polymerization and contraction in airway smooth muscle. J Physiol 596, 3617–3635. [PubMed: 29746010]

Zhang W, Du L & Gunst SJ (2010). The effects of the small GTPase RhoA on the muscarinic contraction of airway smooth muscle result from its role in regulating actin polymerization. Am J Physiol Cell Physiol 299, C298–C306. [PubMed: 20445174]

Zhang W & Gunst SJ (2017). Non-muscle (NM) myosin heavy chain phosphorylation regulates the formation of NM myosin filaments, adhesome assembly and smooth muscle contraction. J Physiol 595, 4279–4300. [PubMed: 28303576]

Zhang W, Huang Y & Gunst SJ (2012). The small GTPase RhoA regulates the contraction of smooth muscle tissues by catalyzing the assembly of cytoskeletal signaling complexes at membrane adhesion sites. J Biol Chem 287, 33996–34008. [PubMed: 22893699]

Zhang W, Huang Y & Gunst SJ (2016). p21-Activated kinase (Pak) regulates airway smooth muscle contraction by regulating paxillin complexes that mediate actin polymerization. J Physiol 594, 4879–4900. [PubMed: 27038336]

Zhang W, Huang Y, Wu Y & Gunst SJ (2015). A novel role for RhoA GTPase in the regulation of airway smooth muscle contraction. Can J Physiol Pharmacol 93, 129–136. [PubMed: 25531582]

Zhang W, Wu Y, Du L, Tang DD & Gunst SJ (2005). Activation of the Arp2/3 complex by N-WASp is required for actin polymerization and contraction in smooth muscle. Am J Physiol Cell Physiol 288, C1145–C1160. [PubMed: 15625304]

Zhang W, Wu Y, Wu C & Gunst SJ (2007). Integrin-linked kinase regulates N-WASp-mediated actin polymerization and tension development in tracheal smooth muscle. J Biol Chem 282, 34568–34580. [PubMed: 17897939]

Keypoints

- S100A4 is expressed in many tissues, including smooth muscle (SM), but its physiologic function is unknown. S100A4 regulates the motility of metastatic cancer cells by binding to non-muscle (NM) myosin II.
- Contractile stimulation causes the polymerization of NM myosin in airway SM, which is necessary for tension development. NM myosin regulates the assembly of adhesion junction signalling complexes (adhesomes) that catalyse actin polymerization.
- In airway SM, ACh (acetylcholine) stimulated the binding of S100A4 to the NM myosin heavy chain, which was catalysed by RhoA GTPase via the RhoA-binding protein, rhotekin. The binding of S100A4 to NM myosin was required for NM myosin polymerization, adhesome assembly and actin polymerization.
- S100A4 plays a critical function in the regulation of airway SM contraction by catalysing NM myosin filament assembly. The interaction of S100A4 with NM myosin may also play an important role in the physiologic function of other tissues.

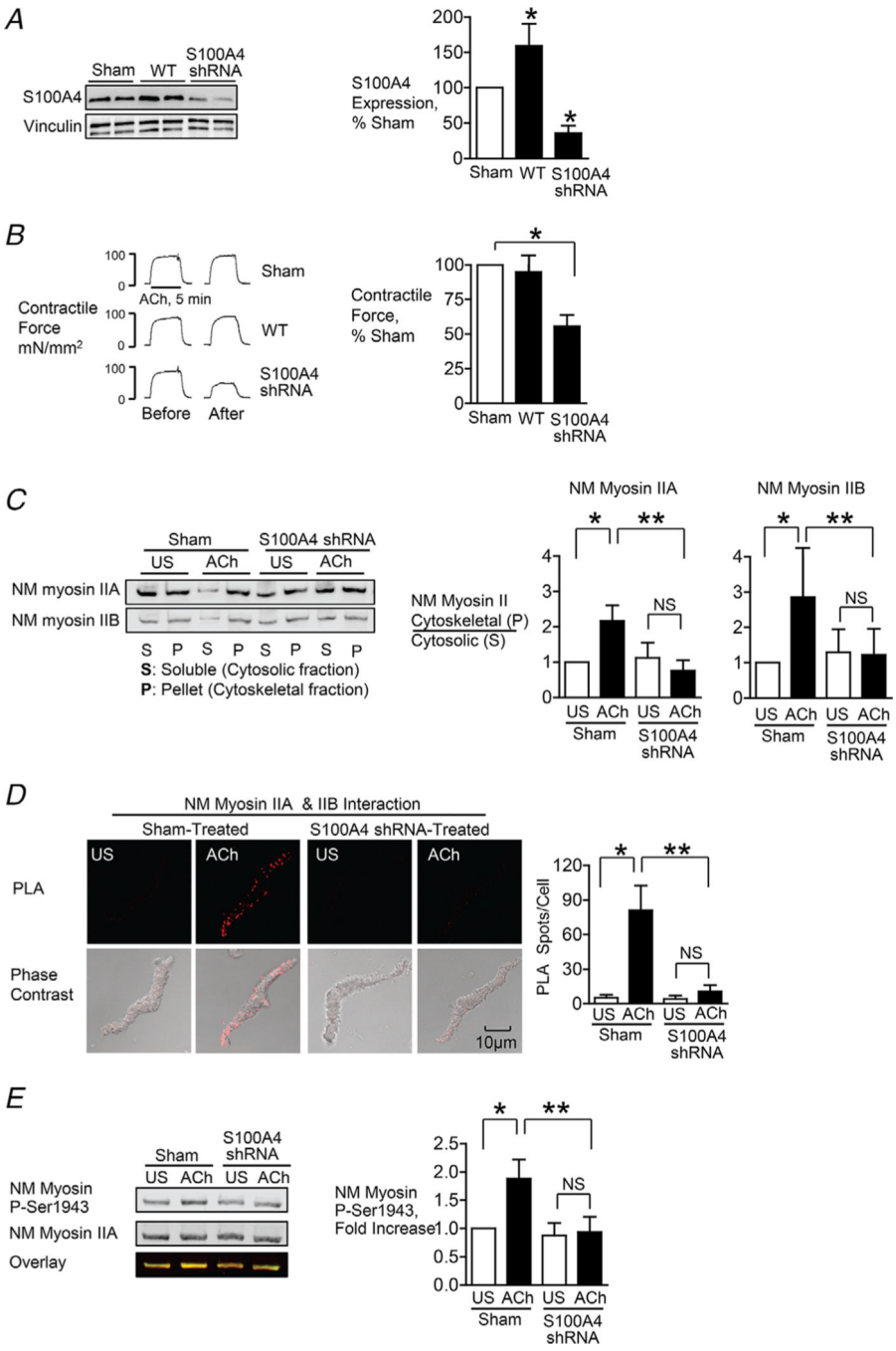

Figure 1. S100A4 depletion inhibits NM myosin II heavy chain assembly and tension development in airway SM tissues in response to contractile stimulation

S100A4 was depleted or overexpressed in tracheal SM tissues using plasmids encoding shRNA or WT S100A4. *A*, typical immunoblots and mean expression levels of S100A4 protein in tracheal SM tissues ($n = 12$, $p = 0.0001$). *B*, contractile force in response to ACh before and after transfection. Depletion of S100A4 significantly inhibited tension development in response to 10^{-5} M ACh ($n = 16$, $p = 0.0001$). *C*, assembly of NM myosin II filaments was significantly inhibited by the depletion of S100A4 in ACh-stimulated tracheal SM tissues (NM myosin IIA, $n = 6$, $p = 0.0001$; NM myosin IIB ($n = 5$, $p = 0.0264$). NM

myosin II assembly was determined by assessing the ratio of NM myosin II in the cytoskeletal (P) *vs.* soluble (S) fractions of tracheal tissue extracts. *D*, assembly of NM myosin II filaments was significantly inhibited by the depletion of S100A4 in ACh stimulated tracheal SM cells. *In situ* PLA fluorescence and PLA fluorescence merged with phase contrast is shown in freshly dissociated SM cells that were unstimulated (US) or stimulated with ACh. PLA fluorescence spots show interactions between NM myosin IIA and NM myosin IIB in cells dissociated from sham-treated tissues and in cells dissociated from tissues after S100A4 depletion. ACh stimulation resulted in a significant increase in the number of complexes between NM myosin IIA and NM myosin IIB at the cell cortex in sham-treated tissues but not in tissues treated with S100A4 shRNA [$n = 16$ (sham) or 17 (shRNA), $p = 0.0001$]. *E*, NM myosin II heavy chain Ser1943 phosphorylation increased significantly in response to 5 min stimulation with 10^{-5} M ACh in sham-treated tissues but not in S100A4 depleted tissues ($n = 11$, $p = 0.0001$). Data were analysed by a paired Student's *t* test (A, B) or by one-way ANOVA with repeated measures (*C*–*E*). Values are the mean ± SD. *Significant difference between unstimulated (US) and ACh stimulated groups. **Significant difference between treatment groups. NS, no significant difference.

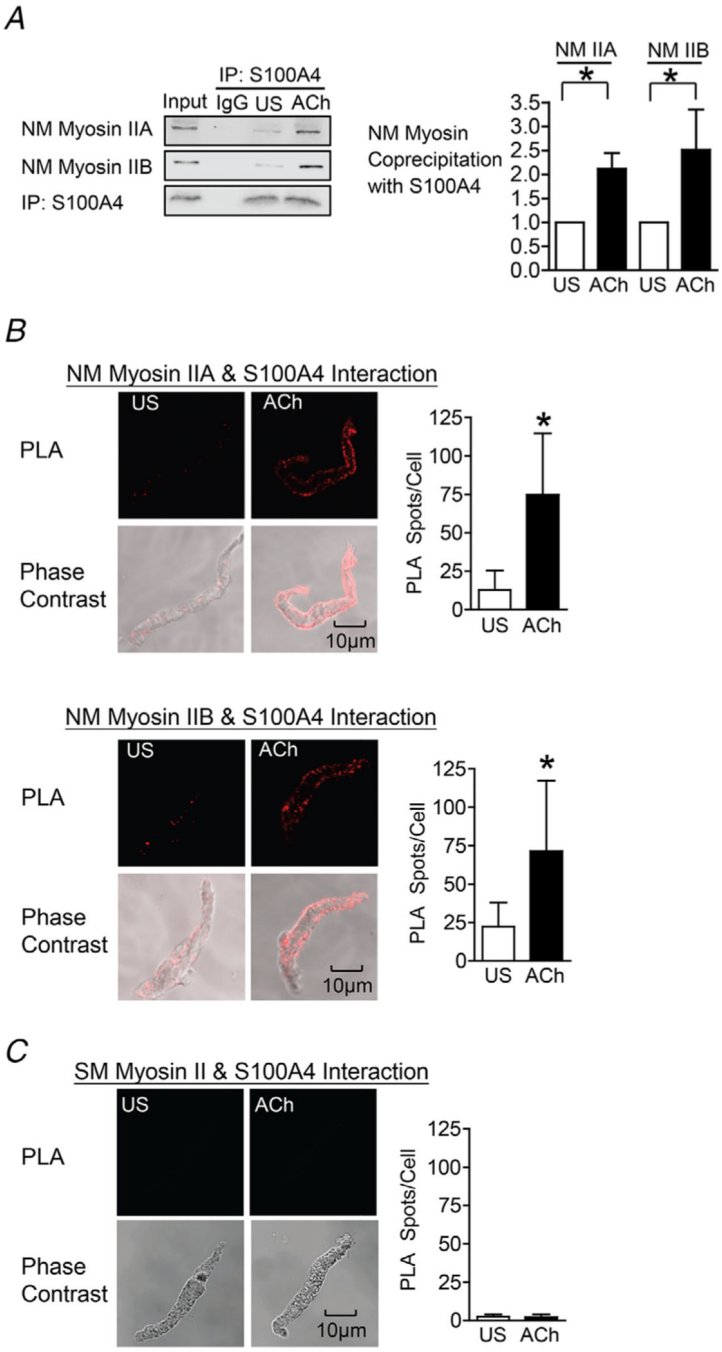

Figure 2. Contractile stimulation results in the interaction of S100A4 with NM myosin II in airway SM

A, S100A4 was immunoprecipitated from extracts of tracheal SM tissues and immunocomplexes were blotted for S100A4 and NM myosin IIA or IIB. Stimulation for 5 min with 10^{-5} M ACh increased the interaction between S100A4 and NM myosin IIA (n = 9, p = 0.0001) and with NM myosin IIB (n = 5, p = 0.0162). *B*, *in situ* PLA was used to determine the interaction of S100A4 and NM myosin IIA or NM myosin IIB in freshly dissociated tracheal SM cells. Stimulation with ACh caused a significant increase in the number of PLA spots representing S100A4/NM myosin II complexes at the cell membrane

(NM myosin IIA: US, $n = 16$ cells; ACh, $n = 16$ cells; $p = 0.0001$. NM myosin IIB: US, $N = 17$ cells; ACh, $n = 16$ cells; $P = 0.0002$). *C*, *in situ* PLA shows the interaction of S100A4 and SM (SM) myosin II. Very few spots were observed in either unstimulated (US) or ACh-stimulated cells ($n = 17$ for each group, $p = 0.3896$). Data analysed by a paired Student's *t* test (*A*) or an unpaired Student's *t* test (*B* and *C*). All values are the mean ± SD. *Significant difference between unstimulated (US) and ACh-stimulated groups.

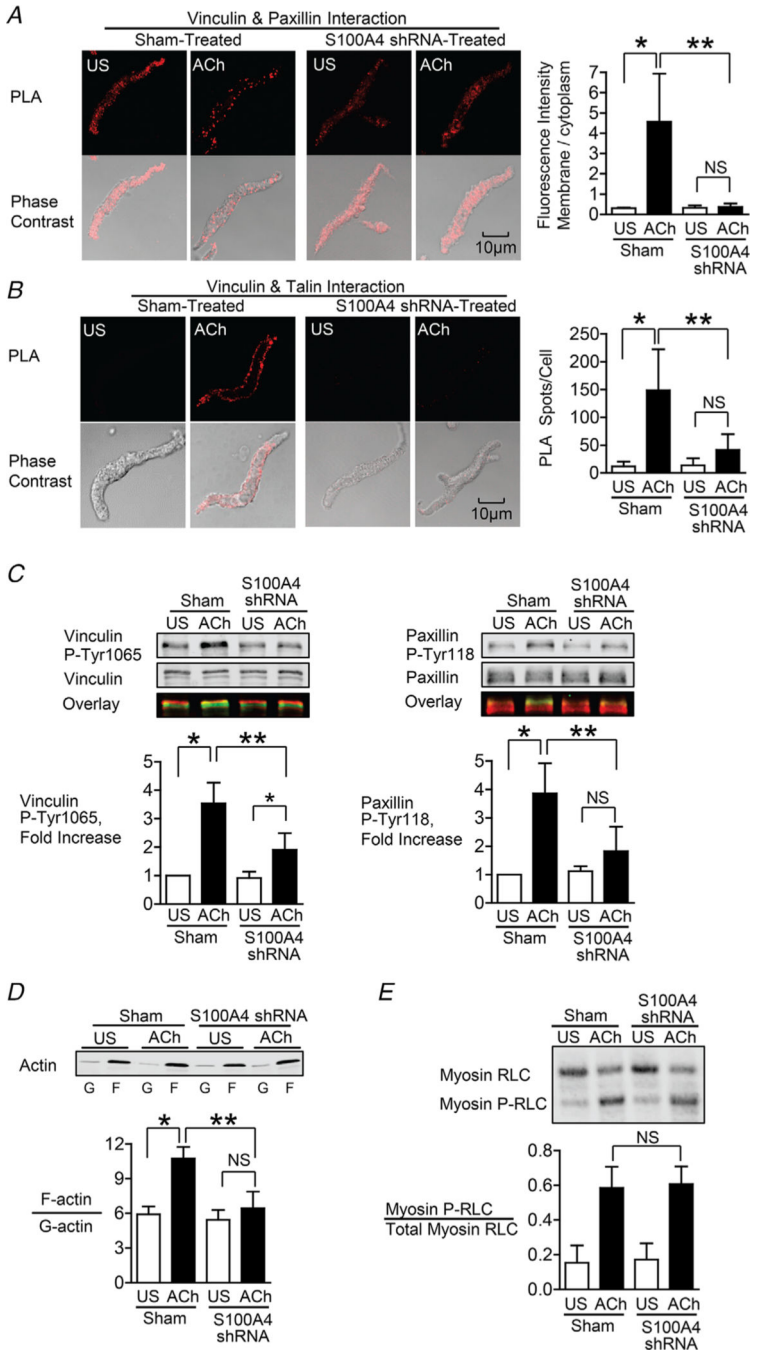

Figure 3. S100A4 depletion inhibits the membrane localization and activation of vinculin and paxillin, and S100A4 depletion inhibits actin polymerization but does not affect myosin RLC phosphorylation

A and *B*, *in situ* PLA fluorescence and PLA fluorescence merged with phase contrast from unstimulated (US) or ACh stimulated cells freshly dissociated from sham-treated or S100A4-depleted tissues. *A*, paxillin–vinculin complexes are distributed throughout the cytoplasm of unstimulated cells from both sham-treated and S100A4-depleted tissues. ACh stimulation resulted the localization of paxillin–vinculin complexes to the membrane of sham-treated cells (US, $n = 13$; ACh, $n = 15$, $p = 0.0001$), whereas paxillin–vinculin

complexes remained distributed throughout the cytoplasm of S100A4-depleted cells (US, n = 12; ACh, n = 14, p = 0.0001). *B*, ACh stimulation resulted in a marked increase in the number of talin–vinculin complexes at the cell membrane in sham-treated cells (US, n = 21; ACh, n = 29, p = 0.0001). S100A4 depletion inhibited the ACh-induced increase of the interaction between talin and vinculin at the cell membrane (US, n = 26; ACh, n = 30, p = 0.0681). Few spots were observed in S100A4-depleted treated cells with or without stimulation. *C*, representative immunoblots from extracts of sham-treated muscle tissues and S100A4 shRNA-treated tissues stimulated with ACh or not stimulated (US). The increases in vinculin Tyr1065 phosphorylation and paxillin Tyr118 phosphorylation in response to 10^{-5} M ACh were significantly inhibited in tissues depleted of S100A4 (n = 6, p = 0.0001). *D*, immunoblot of soluble G-actin (globular) and insoluble F-actin (filamentous) in fractions from extracts of unstimulated (US) or ACh-stimulated muscle tissues treated with S100A4 shRNA or sham-treated. Ratios of F-actin to G-actin were determined by quantitating F and G actin in extracts from each muscle strip. Depletion of S100A4 prevented the increase in the F-actin/G-actin ratio in response to ACh (n = 4, p = 0.0003). *E*, representative immunoblot of unphosphorylated and phosphorylated 20 kDa myosin RLCs from extracts of sham-treated or S100A4 shRNA-treated tissues stimulated with ACh or unstimulated (US). Depletion of S100A4 did not significantly affect myosin RLC phosphorylation in response to ACh (n = 12, p = 0.5317). Myosin RLC phosphorylation was quantified as the ratio of phosphorylated myosin RLC (Myosin P-RLC) to total myosin RLC in each sample. Data are analysed by one-way ANOVA with repeated measures. All values are the mean ± SD. *Significant difference between unstimulated (US) and ACh. **Significant difference between sham and shRNA treatment groups. NS, no significant difference.

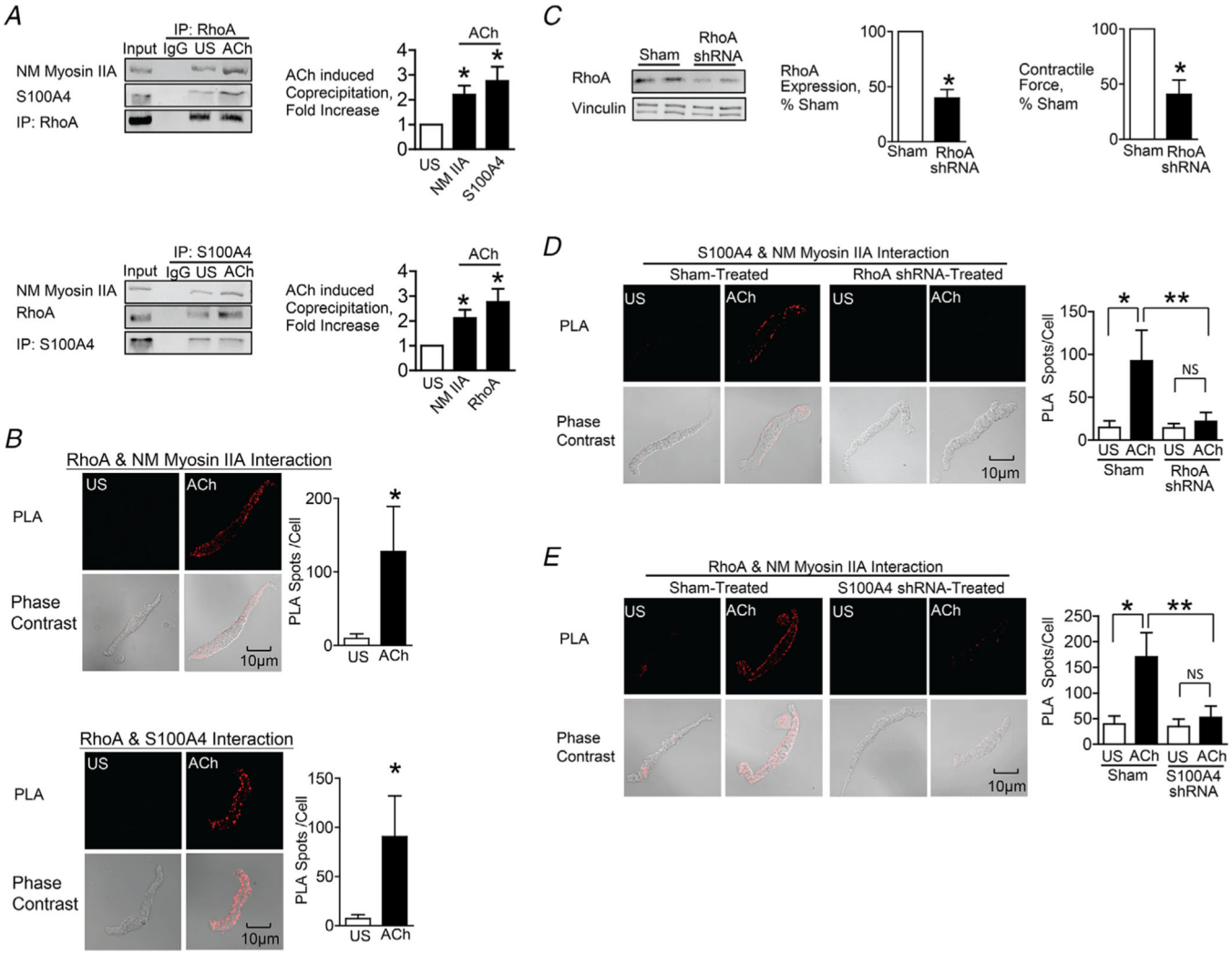

Figure 4. The interaction between S100A4 with NM myosin II in response to ACh is stimulated by the activation of RhoA

A, RhoA or S100A4 was immunoprecipitated from extracts of SM tissues and immunocomplexes were blotted for RhoA, S100A4 and NM myosin IIA. Stimulation for 5 min with 10^{-5} M ACh significantly increased the amount of S100A4 ($n = 6$, $p = 0.0007$) and NM myosin IIA ($n = 4$, $p = 0.0073$) in RhoA immunoprecipitates. ACh stimulation increased the amount of RhoA ($n = 6$, $p = 0.0005$) and NM myosin IIA ($n = 9$, $p = 0.0001$) in S100A4 immunoprecipitates. *B*, *in situ* PLA was used to visualize the interaction of RhoA with NM myosin IIA and of RhoA with S100A4 in freshly dissociated tracheal SM cells. Stimulation with ACh caused a significant increase in the number of PLA spots at the cell membrane (RhoA and NM myosin IIA, $n = 16$ cells for both US and ACh, $p = 0.0001$); S100A4 and RhoA, $n = 19$ for US and $n = 25$ for ACh, $p = 0.0001$). *C*, tracheal SM tissues were depleted of RhoA protein using shRNA and RhoA was quantified in tissue extracts by immunoblotting ($n = 8$, $p = 0.0001$). Depletion of RhoA significantly inhibited tension development in response to 10^{-5} M ACh ($n = 8$, $P < 0.0001$). *D*, PLA was used to visualize interactions between S100A4 and NM myosin IIA in cells dissociated from sham-treated and RhoA-depleted tissues. ACh stimulation of sham-treated cells resulted in a significant

increase in the number of interactions between S100A4 and NM myosin IIA (US, $n = 27$; ACh, $n = 28$, $p = 0.0001$). By contrast, few interactions were observed in cells from RhoA-depleted tissues (US, $n = 26$; ACh, $n = 26$ $p = 0.5018$). RhoA depletion inhibited the ACh-induced increase in interactions between S100A4 and NM myosin IIA ($p = 0.0001$). *E*, PLA shows interactions between RhoA and NM myosin IIA in cells dissociated from sham-treated tissues and S100A4-depleted tissues. ACh stimulation of sham-treated cells resulted in a significant increase in the number of interactions between RhoA and NM myosin IIA. By contrast, few interactions were observed in cells from S100A4-depleted tissues. ($n = 26$ for each group). S100A4 depletion inhibited the ACh-induced increase in the interaction between RhoA and NM myosin IIA ($P = 0.0001$). Data analysed by a paired Student's *t* test (*A* and *C*), an unpaired Student's *t* test (*B*) or by one-way ANOVA (*D* and *E*). All values are the mean ± SD. *Significant difference between US and ACh. **Significant difference between treatment groups. NS, no significant difference.

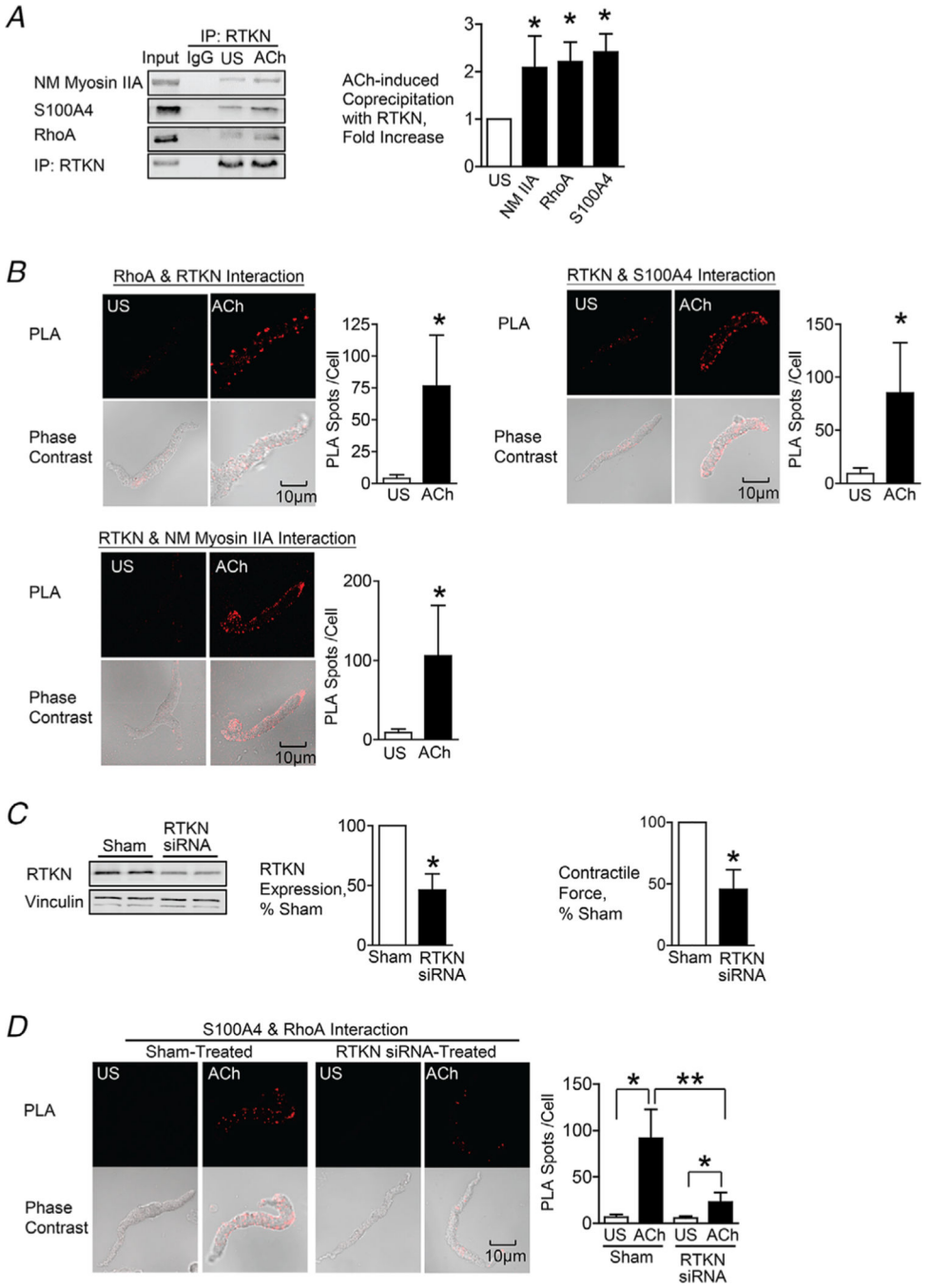

Figure 5. Rhotekin couples RhoA to S100A4 and NM myosin II in SM cells and tissues stimulated with ACh

A, rhotekin (RTKN) was immunoprecipitated from tissue extracts and immunocomplexes were blotted for RhoA, S100A4, RTKN and NM myosin IIA. Stimulation for 5 min with 10^{-5} M ACh significantly increased the coprecipitation of NM myosin IIA ($n = 6$, $p = 0.0070$), RhoA ($n = 3$, $p = 0.0359$) and S100A4 ($n = 9$, $p = 0.0001$) with RTKN. *B*, *in situ* PLA was used to determine the interaction of RTKN and RhoA, S100A4 and NM myosin IIA in freshly dissociated tracheal SM cells. Stimulation with ACh caused a significant increase in the number of PLA complexes between all four proteins (RTKN-RhoA, $n = 20$, p

= 0.0001; RTKN-S100A4, $n = 20$, $p = 0.0001$; RTKN-NM myosin IIA, $n = 31$, $p = 0.0001$). *C*, tracheal SM tissues were treated with RTKN siRNA. Depletion of RTKN significantly inhibited protein expression ($n = 10$, $p = 0.0001$) and also inhibited tension development in response to 10^{-5} M ACh stimulation ($n = 16$, $p = 0.0001$). *D*, PLA shows interactions between S100A4 and RhoA in cells dissociated from sham-treated tissues and from RTKN-depleted tissues. ACh stimulation of sham-treated cells resulted in a significant increase in the interactions between S100A4 and RhoA (US, $n = 16$; ACh, $n = 20$). RTKN depletion inhibited the ACh-induced increase of the interaction between S100A4 and RhoA ($p = 0.0001$) (US, $n = 18$; ACh, $n = 19$). Data analysed by a paired Student's *t* test (*A* and *C*), an unpaired Student's *t* test (*B*) or by one-way ANOVA (*D*). All values are the mean ± SD. *Significant difference between US and ACh; **Significant difference between treatment groups ($P < 0.05$); NS, no significant difference.

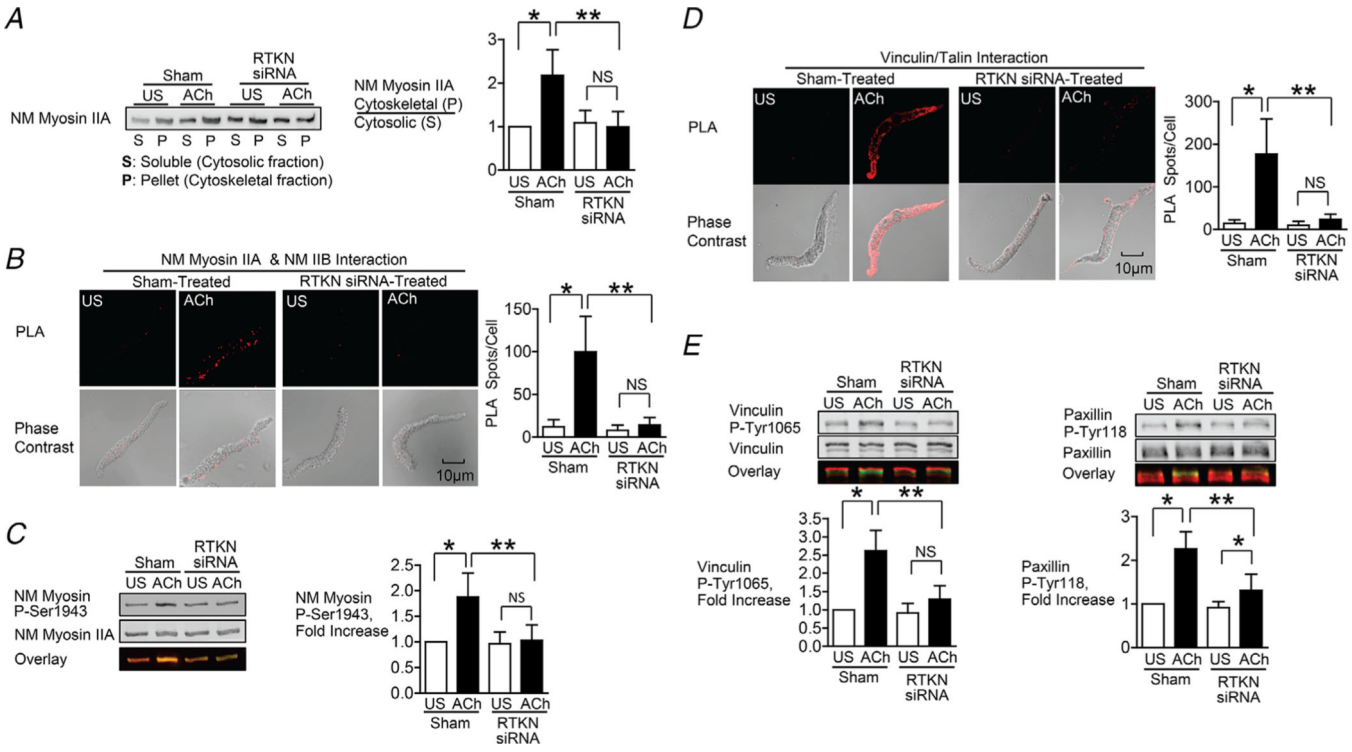

Figure 6. Depletion of rhotekin inhibits NM myosin II polymerization and membrane recruitment and activation of vinculin and paxillin in response to Ach

A, immunoblot of NM myosin II in cytoskeletal (P) and soluble (S) fractions from extracts of tracheal SM tissues treated with RTKN siRNA or untreated (Sham) and stimulated for 5 min with 10^{-5} M ACh or unstimulated (US). RTKN depletion significantly inhibited the ACh-induced increase in the ratio of NM myosin II in the cytoskeletal (P) *vs.* soluble (S) fractions ($n = 6$, $p = 0.0001$). *B*, *in situ* PLA fluorescence in freshly dissociated US or ACh-stimulated SM cells from sham-or siRNA-treated tracheal SM tissues. ACh stimulation of sham-treated tissues resulted in a significant increase in the number of NM myosin IIA and IIB complexes at the cell cortex ($n = 20$ cells/group). RTKN depletion inhibited the ACh-induced increase in the interaction between NM myosin IIA and IIB ($n = 20$ cells/group, $P = 0.0001$). *C*, RTKN depletion significantly inhibited the increase in NM myosin II Ser1943 phosphorylation in tracheal muscle tissues in response to 5 min stimulation with 10^{-5} M ACh ($n = 11$, $P = 0.0001$). *D*, *in situ* PLA fluorescence shows interactions between talin and vinculin in US or ACh-stimulated freshly dissociated SM cells from sham-treated or RTKN-depleted tissues. ACh stimulation resulted in a significant increase in the number of talin-vinculin complexes at the cell membrane (US cells, $n = 19$; ACh, $n = 25$ cells, $p = 0.0001$). RTKN depletion inhibited the ACh-induced increase in the interaction between talin and vinculin (US, $n = 18$; ACh, $n = 20$, $p = 0.0001$). *E*, immunoblots of extracts from sham-treated and RTKN-siRNA treated tissues stimulated with Ach or US. The increase in vinculin Tyr1065 phosphorylation and paxillin Tyr118 phosphorylation in response to Ach was significantly inhibited in tissues with rhotekin depletion ($n = 9$, $p = 0.0001$). Data analysed by one-way ANOVA. All values are means ± SD. *Significant difference between US and ACh; **significant difference between treatment groups; NS, no significant difference.

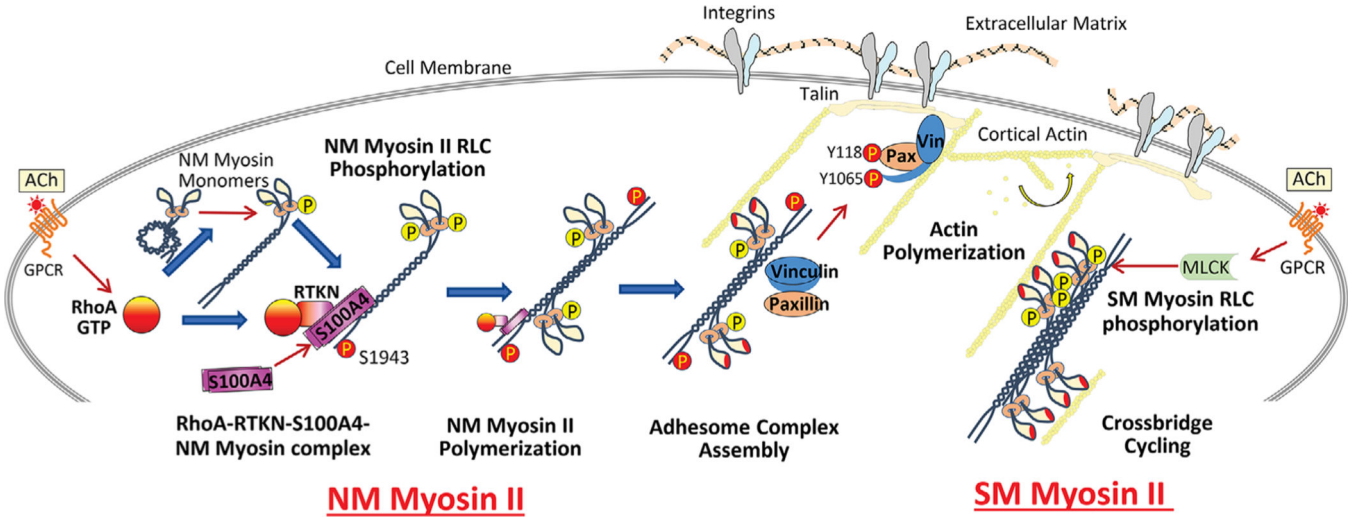

Figure 7. Model for proposed role of S100A4 in the regulation of NM myosin II filament assembly and contractile tension development in airway SM

The activation of RhoA GTPase by ACh catalyses the binding of S100A4 to the C-terminal heavy chain of assembly-competent NM myosin II monomers at the cell cortex via the RhoA GTP-binding protein, rhotekin. S100A4 binding facilitates the polymerization of NM myosin II monomers into filaments. RhoA also regulates the phosphorylation of the RLC of NM myosin II, which promotes the assembly-competent conformation of NM myosin II and also activates actin-activated cross-bridge cycling by NM myosin II filaments. Cross-bridge cycling by NM myosin II provides the motor for the recruitment of the adhesome proteins vinculin and paxillin to integrin-associated adhesome complexes at the membrane. Signalling pathways activated by these complexes regulate cortical actin polymerization, which is necessary for tension generation. Concurrently, the activation of cross-bridge cycling by SM myosin II regulates tension generation by the SM contractile apparatus.